Light propagation in a birefringent plate with topological charge

Ebrahim Karimi,[1,2] Bruno Piccirillo,[1] Lorenzo Marrucci,[1,2] and Enrico Santamato[1,*]

[1]*Dipartimento di Scienze Fisiche, Università degli Studi di Napoli "Federico II," Complesso di Monte S. Angelo, via Cintia, 80126 Napoli, Italy*

[2]*Consiglio Nazionale delle Ricerche-INFM Coherentia, 80126 Napoli, Italy*

**Corresponding author: enrico.santamato@na.infn.it*

Received December 2, 2008; accepted March 3, 2009;
posted March 16, 2009 (Doc. ID 104697); published April 8, 2009

We calculated the Fresnel paraxial propagator in a birefringent plate having topological charge q at its center, named "q-plate." We studied the change of the beam transverse profile when it traverses the plate. An analytical closed form of the beam profile propagating in the q-plate can be found for many important specific input beam profiles. We paid particular attention to the plate having a topological unit charge and found that if small losses due to reflection, absorption, and scattering are neglected, the plate can convert the photon spin into orbital angular momentum with up to 100% efficiency provided the thickness of the plate is less than the Rayleigh range of the incident beam. © 2009 Optical Society of America

OCIS codes: 050.1960, 260.1960, 260.6042.

Light beams carrying orbital angular momentum (OAM) are receiving increasing attention as a resource in quantum and classical optics, since OAM exists in an inherently multidimensional space. Information can thus be encoded in higher dimensional OAM alphabets [1,2] for its use in free-space communication systems [3] or to increase the dimensionality of the working Hilbert space in quantum communications systems [4]. The main characteristics of a light beam carrying OAM is the presence of a topological point-charge of integer order in the optical phase. It was recently demonstrated that a birefringent plate made of a vortex-patterned liquid crystal film can imprint its topological charge into the optical phase of the incident light, thus changing the OAM of the beam. Being birefringent, the plate affects the photon spin angular momentum (SAM) also, thus providing easy control of the beam OAM content by either changing its polarization or changing the retardation of the plate [5]. It can be shown that if the topological charge of the birefringent plate is q, the OAM of a light beam passing through such a "q-plate" (QP) changes by an amount $\pm 2q\hbar$ per photon. One may roughly think of the QP as of an ordinary birefringent plate rotated at angle α about the beam z axis with α given by $\alpha=\alpha(x,y)=\arctan(y/x)=\phi$, where ϕ is the azimuthal angle in the x,y plane. This simple picture is enough to account for some qualitative effects, such as, for instance, the SAM-to-OAM conversion (STOC) [5], the associated optical Berry phase [6], and the changes of the SAM and OAM content of the beam at different depths in the QP [7] but cannot be used to determine the detailed quantitative behavior of the beam during its propagation. In fact, the formal replacement $\alpha\rightarrow\phi(x,y)$ is justified only if the function $\alpha(x,y)$ varies smoothly over the optical wavelength scale [the so-called geometric optics approximation (GOA)] [7], which is not true in the present case, because no length scale is defined by the function $\arctan(y/x)$. As shown below, an exact series solution of the wave equation inside the QP shows that all field and wave propagators at the QP singularity vanish, which is not true for fields [5] and propagators [7] calculated by just setting $\alpha\rightarrow\phi$. To overcome this broad discrepancy, in this Letter, we study the propagation of a light beam in the QP without having recourse to the GOA but assuming, instead, a good beam paraxiality. We start from Maxwell's wave equation $\nabla^2\mathbf{E}-\nabla(\nabla\cdot\mathbf{E})+k_0^2\hat{\epsilon}\cdot\mathbf{E}=0$, where $k_0=2\pi/\lambda=\omega/c$; $\hat{\epsilon}$ is the relative dielectric tensor at frequency ω, c is the speed of light, and λ is the wavelength. The relative dielectric tensor is given by $\hat{\epsilon}=\hat{R}(q\phi)\cdot\hat{\epsilon}_{\mathrm{local}}\cdot\hat{R}(-q\phi)$, where $\hat{\epsilon}_{\mathrm{local}}=\mathrm{diag}(n_o^2,n_e^2,n_o^2)$ is the dielectric tensor in the local frame of the plate, $\hat{R}(\alpha)$ is the rotation matrix about the z axis, ϕ is the azimuthal angle, and n_o and n_e are the material ordinary and extraordinary indices, respectively. We neglect absorption and assume positive birefringence $n_e>n_o$. In most materials, including liquid crystals, the birefringence is small, $(n_e-n_o)\ll n_o$, so that we may neglect the longitudinal part of the optical field and take $\nabla\cdot\mathbf{E}\simeq 0$. In this approximation, the wave equation reduces to Helmholtz's vector equation $\nabla^2\mathbf{E}_\perp+k_0^2\hat{\epsilon}\cdot\mathbf{E}_\perp=0$ for the transverse part $\mathbf{E}_\perp$ of the field. In view of the cylindrical symmetry of the problem, it is convenient to find the eigenmodes of the Helmholtz's vector equation in the circular polarization basis $E_\pm=(E_x\pm iE_y)/\sqrt{2}$ and in the cylindrical coordinates (r,ϕ,z) by setting $\mathbf{E}_\perp(r,\phi,z)=(\mathrm{E}_+(r)e^{i(m+q)\phi},\mathrm{E}_-(r)e^{i(m-q)\phi},0)e^{-ik_0\gamma z+i\omega t}$, where γ is the longitudinal spatial frequency and $z=0$ is the input-face of the QP. Inserting this field into Helmholtz's equation yields a pair of coupled radial equations,

$$f''(r)+\frac{f'(r)}{r}+\left(k_0^2(n_o^2-\gamma^2)-\frac{\mu^2}{r^2}\right)f(r)=\frac{\nu g(r)}{r^2},$$

$$g''(r)+\frac{g'(r)}{r}+\left(k_0^2(n_e^2-\gamma^2)-\frac{\mu^2}{r^2}\right)g(r)=\frac{\nu f(r)}{r^2}, \quad (1)$$

where $f(r)=(E_+ + E_-)/\sqrt{2}$, $g(r)=(E_+ - E_-)/\sqrt{2}$, $\mu=\sqrt{m^2+q^2}$, and $\nu=2mq$. Equations (1) are exact and can be solved by a series. We postpone a full discussion about their solutions to a future work. Here we consider only the approximate solutions for paraxial beams at normal incidence. Setting $\gamma=\gamma_o=\sqrt{n_o^2-\beta^2}\simeq n_o-\beta^2/2n_o$, where β is a transverse spatial spectrum, Eqs. (1) reduce to the equations for the ordinary wave,

$$f_o''(r)+\frac{f_o'(r)}{r}+\left(k_0^2\beta^2-\frac{\mu^2}{r^2}\right)f_o(r)=\frac{\nu g_o(r)}{r^2},$$

$$g_o''(r)+\frac{g_o'(r)}{r}+\left(k_0^2\beta^2\Lambda^2-\frac{\mu^2}{r^2}\right)g_o(r)=\frac{\nu f_o(r)}{r^2}, \quad (2)$$

where $\Lambda^2=1+2(n_e^2-n_o^2)/\beta^2$. We observe that in commercial liquid crystals we have $n_e^2-n_o^2\simeq 0.5$, while usual paraxial laser beams at normal incidence have the radial spatial frequency with β ranging from zero to $\beta\simeq 10^{-2}$. The parameter Λ^2 is therefore very large in all practical cases. We may then solve Eqs. (2) as an asymptotic series of Λ^2. The zero-order approximation of the asymptotic solution of Eq. (2) for the ordinary wave is given by $f_o(r)=A_oJ_\mu(k_0\beta r)$ and $g_o(r)=0$, where A_o is an arbitrary constant and $J_\mu(x)$ is Bessel's function of index $\mu=\sqrt{m^2+q^2}$. The differential equation for the extraordinary wave is obtained from Eqs. (1) by setting $\gamma=\gamma_e=\sqrt{n_e^2-\beta^2}\simeq n_e-\beta^2/2n_e$, and it can be obtained from Eqs. (2) by the formal replacements $f\to g$, $g\to f$, $\Lambda^2\to-\Lambda^2$. The zero-order asymptotic solution for the extraordinary wave is then given by $f_e(r)=0$ and $g_e(r)=A_eJ_\mu(k_0\beta r)$ with constant A_e. All other terms of the asymptotic solution can be found recursively. The zero-order asymptotic solutions hold in the whole x, y plane except a small region about the origin having a radius $r_0\approx\lambda/(\Lambda\beta)=\lambda/\sqrt{n_e^2-n_o^2}$. For commercial liquid crystal we have $r_0\approx 1.25\lambda$. In this small region is located the singularity, and the optical axis is not well defined here. The effect of this region can be accounted for only by the exact (not paraxial) wave approach, but we may anticipate on physical grounds that the main effect of this region is to scatter a small fraction of the light at large angles out of the paraxial beam. From the asymptotic paraxial modes of Helmholtz's equation it is straightforward to calculate the Fresnel paraxial propagator for the optical field $\mathbf{E}_\perp$. The optical field at plane z in the QP is given by

$$\mathbf{E}_\perp(r,\phi,z)=\frac{1}{2}\int_0^\infty \rho d\rho\int_0^{2\pi} d\psi\hat{R}(q\phi)\{(K^o+K^e)\hat{1}+(K^o-K^e)\hat{\sigma}_z\}\hat{R}(-q\psi)\mathbf{E}_\perp(\rho,\psi,0), \quad (3)$$

where $\hat{1}$, $\hat{R}(\phi)$, and $\hat{\sigma}_z$ are the 2×2 unit, rotation, and Pauli's matrices, respectively. The Fresnel kernels in Eq. (3) are given by $K^{o,e}=\Sigma_m K^{o,e}_{\mu(m)}(r,\rho;z)e^{im(\phi-\psi)}$, where $\mu(m)=\sqrt{m^2+q^2}$ and

$$K^{o,e}_{\mu(m)}(r,\rho;z)=\left(\frac{in_{o,e}k_0}{2\pi z}\right)i^{\mu(m)}J_{\mu(m)}\left(\frac{k_0n_{o,e}r\rho}{z}\right)\times e^{-ik_0n_{o,e}(r^2+\rho^2)/2z-ik_0n_{o,e}z}. \quad (4)$$

The Fresnel kernels K^o and K^e in Eq. (4) are characterized by the presence of a Bessel function of irrational order. Although K^o and K^e cannot be obtained in a closed form, they permit one to evaluate analytically the field transmitted by the QP in important cases, such as, for instance, Laguerre–Gauss incident beams. Here we consider only the case of an LG_{0l} beam impinging onto the QP. Setting $\mathbf{E}_\perp(\rho,\phi,0)=e^{il\phi}LG_0^l(\rho)\begin{bmatrix}a\\b\end{bmatrix}$ in the circular polarization basis, where $LG_0^l(\rho)$ is the radial amplitude of Laguerre–Gauss modes, we obtain

$$\begin{bmatrix}E_+\\E_-\end{bmatrix}=e^{i(l\phi-k_0n_oz)}\begin{bmatrix}K^+_{\mu^-} & K^-_{\mu^+}e^{2iq\phi}\\ K^-_{\mu^-}e^{-2iq\phi} & K^+_{\mu^+}\end{bmatrix}\begin{bmatrix}a\\b\end{bmatrix}, \quad (5)$$

where $K^\pm_\mu=(HyGG_{|l|-\mu,\mu}(r,z/n_o)\pm e^{-ik_0\Delta nz}HyGG_{|l|-\mu,\mu}\times(r,z/n_e))/2$, $\Delta n=n_e-n_o$, $\mu^\pm=\mu(\ell\pm q)$, and $HyGG_{p,m}(r,z)$ is the Hypergeometric–Gaussian mode [8], viz.,

$$HyGG_{pm}(\rho,\zeta)=C_{pm}\zeta^{p/2}(\zeta+i)^{-(1+|m|+p/2)}\rho^{|m|}\times e^{-i\rho^2/(\zeta+i)}{}_1F_1\left(-\frac{p}{2},1+|m|;\frac{\rho^2}{\zeta(\zeta+i)}\right), \quad (6)$$

where

$$C_{pm}=i^{|m|+1}\sqrt{2^{p+|m|+1}/\pi\Gamma(p+|m|+1)}\Gamma(1+|m|+p/2)/\Gamma(|m|+1),$$

$\rho=r/w_0$, $\zeta=z/z_R$, and $z_R=k_0w_0^2/2$ is the beam Rayleigh range. Because $n_o\simeq n_e$, the arguments of the function $HyGG_{pm}$ in Eq. (5) are very close so that when $\Delta nz=j\lambda$ ($j=1,2,\ldots$) the matrix in Eq. (5) is almost diagonal; the beam in the QP has the same value of OAM, i.e., $\ell\hbar$ per photon. When $\Delta nz=(2j-1)\lambda/2$, instead, only the off-diagonal elements survive; the right and the left circular components of the transmitted field assume a phase factor $e^{\pm 2iq\phi}$ and the

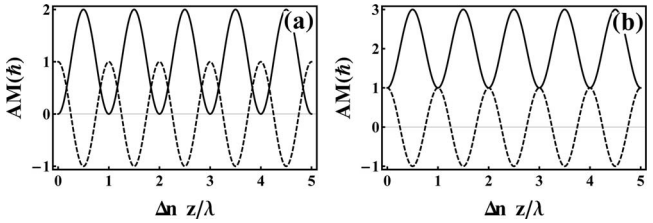

Fig. 1. Beating of SAM (dashed curve) and OAM (solid curve) as a function of the optical retardation $\Delta nz/\lambda$ while a circularly polarized input beam propagates in the 1-plate. (a) For LG_{00} and (b) LG_{01} as an input beam. We used the following data: $n_o=1.5$, $n_e=1.7$, and $w_0=50\lambda$.

beam OAM change by $\pm 2q\hbar$ per photon, depending on the input circular polarization helicity. As the beam propagates in the QP, its transverse profile, spin, and OAM change. From Eq. (5), we may calculate the average SAM and OAM carried by the beam at the plane z in the QP, obtaining

$$S_z(z) = \frac{1}{\omega}\Re[e^{-ik_0\Delta nz}(|b|^2 I_{|\ell|-\mu^+,\mu^+}(z) - |a|^2 I_{|\ell|-\mu^-,\mu^-}(z))], \tag{7}$$

$$L_z(z) + \frac{q}{\omega}S_z(z) = \frac{1}{\omega}((\ell - q)|a|^2 + (\ell + q)|b|^2), \tag{8}$$

where

$$I_{p,m}(\zeta) = \frac{2^{p+|m|+1}\Gamma^2\left(\frac{p}{2} + |m| + 1\right)}{\Gamma(|m|+1)\Gamma(p+|m|+1)}\chi^{-p/2}(\zeta) \times \left(\frac{n_o n_e}{2n_o n_e - i(n_e - n_o)\zeta}\right)^{p+|m|+1} \times {}_2F_1\left(-\frac{p}{2}, -\frac{p}{2}; |m|+1; \chi(\zeta)\right), \tag{9}$$

and $\chi(\zeta) = \{n_e n_o/[n_e n_o - i(n_e - n_o)\zeta]\}^2$. As expected, we have $I_{p,m}(0) = 1$ so that Eqs. (8) and (7) yield $S_z(0) = (|b|^2 - |a|^2)/\omega$ and $L_z(0) = (|a|^2 + |b|^2)\ell/\omega$. In Fig. 1 the photon STOC [5] is shown as a function of the propagation depth in the 1-plate for LG_{00} and LG_{01} input beams. The conversion efficiency is practically 100%, and its maximum occurs at optical retardation $\Delta nz = (2j-1)\lambda/2$ with integer j. When the optical retardation is $j\lambda$, no conversion occurs and the beam has no OAM. Changing the optical retardation of the 1-plate provides a good way to control the STOC process. However, when the thickness of the 1-plate becomes very large (much larger than the beam Rayleigh range) the conversion efficiency slowly decays. According to Eqs. (5) and (6), the field profile inside the 1-plate (and at its exit face) vanishes as $r^{\sqrt{2}}$ along the beam axis so that the intensity profile has the characteristic doughnut shape irrespective of the OAM carried by the beam. Figure 2 shows the intensity profiles for (a) full STOC and (b) no STOC. For the sake of comparison, the results obtained in the GOA

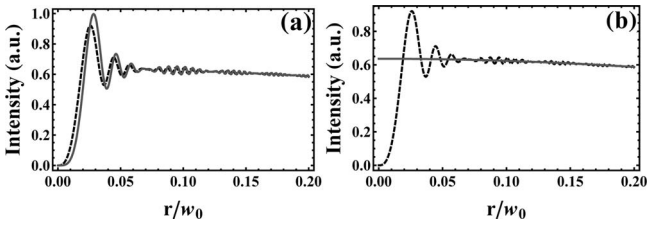

Fig. 2. Intensity profile for (a) full STOC and (b) no STOC in the 1-plate. Solid and dashed curves are simulated by [7] and our theory, respectively. The input beam assumed the TEM_{00}.

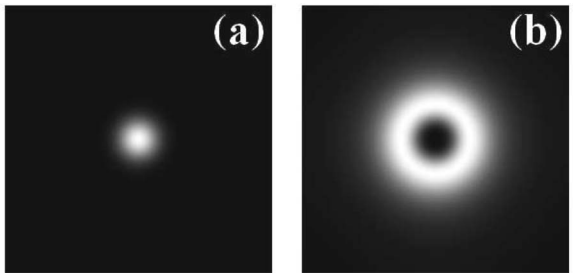

Fig. 3. Intensity profile in the far-field beyond the 1-plate after free-air propagation. (a) No STOC, (b) full STOC.

[7] are also shown. We can deduce that the GOA approximation is fairly good for the case of full STOC but is very bad in the near field and in the case of no STOC. Dramatic changes of the intensity profile depending on the final OAM are seen, however, in the far-field after free-air propagation. When the STOC is maximum, in fact, we observe the doughnut profile, while when no conversion occurs, the far-field pattern has again a maximum at its center. This is shown in Fig. 3.

In conclusion, we calculated the Fresnel propagator of an optical beam in a birefringent plate having a topological charge q in the paraxial approximation and for normal incidence. We considered in some of the details the propagation of an $LG_{0\ell}$ beam in the QP. As the beam traverses the plate, its transverse profile changes from Laguerre–Gaussian to Hypergeometric–Gaussian and STOC occurs. We paid particular attention to the 1-plate and found that the conversion efficiency is almost 100% when the thickness of the plate is much smaller than the beam Rayleigh range and slowly decreases when the thickness of the 1-plate is increased. The free propagation of the HyGG modes generated by the QP is not stable, and the characteristic transition from dot-to-doughnut profile when the OAM changes from 0 is observed only in the far-field. The possibility offered by the azimuthally oriented plate in manipulating entanglement among several degrees of freedom of the light may be of great interest for quantum information, quantum communications, and quantum computing.

References

1. G. Molina-Terriza, J. P. Torres, and L. Torner, Phys. Rev. Lett. **88**, 013601 (2002).
2. G. Molina-Terriza, J. P. Torres, and L. Torner, Nat. Phys. **3**, 305 (2007).
3. G. Gibson, J. Courtial, M. J. Padgett, M. Vasnetsov, V. Pasko, S. M. Barnett, and S. Franke-Arnold, Opt. Express **12**, 5448 (2004).
4. A. Mair, A. Vaziri, G. Welhs, and A. Zeilinger, Nature **412**, 313 (2001).
5. L. Marrucci, C. Manzo, and D. Paparo, Phys. Rev. Lett. **96**, 163905 (2006).
6. L. Marrucci, C. Manzo, and D. Paparo, Appl. Phys. Lett. **88**, 221102 (2006).
7. G. F. Calvo and A. Picón, Opt. Lett. **32**, 838 (2007).
8. E. Karimi, G. Zito, B. Piccirillo, L. Marrucci, and E. Santamato, Opt. Lett. **32**, 3053 (2007).